Characterization of mAb104, a mAb Targeting a Conformationally Exposed, Tumor-Specific Epitope of HER2

Sagun Parakh[1,2,3], Nhi Huynh[1], Diana Dong Cao[1], Angela Rigopoulos[1], Benjamin Gloria[1], Ingrid J.G. Burvenich[1,3], Carmel Murone[1], Christian W. Wichmann[1,3], Nancy Yanan Guo[1], Clare Senko[1,2], Adam Parslow[1], Laura Allan[1], Laura D. Osellame[1,3], Peter W. Janes[1,3], Fiona E. Scott[1], Zhanqi Liu[1], Hui K. Gan[1,2,3,4], and Andrew M. Scott[1,3,4,5]

ABSTRACT

We generated a novel HER2 mAb104, which binds to an epitope in domain II of HER2 that is conformationally exposed in tumors in response to *HER2* amplification or activation but is not accessible to antibody binding in normal tissues. Consistent with other studies that evaluated antibodies targeting conformationally exposed epitopes, mAb104 lacked *in vitro* activity but showed potent antitumor activity *in vivo*. The antitumor effect *in vivo* was similar in magnitude to trastuzumab and pertuzumab, and combination with trastuzumab was superior to trastuzumab alone. IHC screening of normal and tumor tissues with mAb104 showed that mAb104 did not bind to normal tissues, confirming the tumor specificity of mAb104. *In vivo* biodistribution and imaging data demonstrated specific tumor targeting of mAb104 in HER2-expressing tumors. Confocal microscopy clearly demonstrated the internalization of mAb104 into the tumor cells, consistent with mAb104:HER2 trafficking. mAb104 is tumor-specific, exhibits potent antitumor activity in HER2-positive models, and internalizes into HER2-positive tumor cells. These results demonstrate the potential of mAb104 as a novel HER2-targeting therapy, both as a naked antibody for signaling abrogation therapy and for payload delivery as an antibody–drug conjugate or for β/α particle therapy.

Introduction

Many improvements in cancer treatment in the last decade have come from more selective agents that specifically target cancer-associated proteins. One family of such agents targets the ErbB family. The ErbB family of protein kinases comprises four cell surface receptors: EGFR (also known as ErbB1 or HER1), ErbB2 (also known as HER2; *Neu*), ErbB3 (or HER3), and ErbB4 (or HER4; ref. 1). Although lacking specific endogenous ligands, the natural conformation of HER2 favors homo- or heterodimeric interactions between monomeric ErbB family members, as well as oligomerization of preexisting inactive dimers, leading to the autophosphorylation of intracellular kinase domains and signal transduction (2, 3). HER2 overexpression has been observed in many epithelial tumors, usually correlating with malignant transformation, tumor growth, the development of antiapoptotic properties, increased invasiveness, and drug resistance (4–7). A number of therapies targeting HER2 have been tested in clinics, of which the preeminent example is trastuzumab. Trastuzumab binds to the extracellular domain (ECD) IV of HER2 and is the cornerstone of treatment for HER2-positive breast cancer and the only approved biological therapeutic to show a survival benefit in advanced gastric cancer. Another HER2 antibody, pertuzumab, is the first in a class of agents known as HER dimerization inhibitors; pertuzumab binds to the extracellular dimerization domain II of HER2 and inhibits dimerization with other HER receptors (8). Although other anti-HER2 antibodies targeting the ECD have been described (9–11), none have been successful in advancing into routine clinical use yet.

We have previously developed a novel class of antibodies that target conformationally exposed epitopes on the EGFR in tumor-specific conditions, such as when the EGFR is overexpressed, mutated, or in ligand-activated forms. The most advanced of these is mAb806 (12, 13). ABT-806, the humanized form of mAb806, has been shown to be tumor-specific, well tolerated, and devoid of conventional anti-EGFR toxicities (14–16). In view of the tumor-specific targeting of mAb806, an antibody–drug conjugate (ADC) was developed, depatuxizumab mafodotin (ABT-414, AbbVie; ref. 17), comprising mAb806 linked to a cytotoxic payload of monomethyl auristatin F. After confirming its safety in phase I studies (18, 19), depatuxizumab mafodotin was evaluated in a large phase III trial in patients with newly diagnosed glioblastoma (GBM; INTELLANCE I; NCT 02573324; ref. 20) as well as in the phase II INTELLANCE 2/EORTC trial (NCT02343406) in patients with recurrent GBM (21, 22). In addition, next-generation versions of mAb806-based ADCs are being evaluated in early-phase clinical trials (NCT02365662, NCT03234712, and NCT04721015; refs. 23–25).

We have now generated novel first-in-class anti-HER2 mAbs, which target a conformationally exposed epitope in HER2. The binding of these novel antibodies requires a conformational change that occurs upon receptor activation, in which disulfide bonds of domain II of the HER2 receptor can be formed and broken dynamically (12, 13). Exposure of this epitope occurs in tumor-specific conditions; for example, overexpression of HER2 leads to the nonphysiological exposure of the epitope. In this paper, we describe the characteristics and therapeutic potential of our lead candidate, mAb104. In addition, correlative pharmacodynamic studies were

[1]Tumour Targeting Laboratory, Olivia Newton-John Cancer Research Institute, Melbourne, Australia. [2]Department of Medical Oncology, Austin Health, Melbourne, Australia. [3]School of Cancer Medicine, Latrobe University, Melbourne, Australia. [4]Department of Medicine, University of Melbourne, Melbourne, Australia. [5]Department of Molecular Imaging and Therapy, Austin Health, Melbourne, Australia.

Corresponding Author: Andrew M. Scott, Tumour Targeting Laboratory, Olivia Newton-John Cancer Research Institute, 145 Studley Road, Heidelberg 3084, Australia. E-mail: andrew.scott@onjcri.org.au

Mol Cancer Ther 2025;24:1442–52

doi: 10.1158/1535-7163.MCT-24-0583

undertaken to explore treatment effects, and biodistribution studies with zirconium-89 (^{89}Zr)–labeled mAb104 were performed to determine the tumor specificity, normal tissue distribution, and imaging characteristics of mAb104.

Materials and Methods

Hybridoma clones were generated, producing novel mAbs against a conformationally exposed region of the HER2 ECD that was thought to be available for binding only under conditions found in tumor cells. These mAbs were generated to target a conformational epitope through the immunization of mice with the peptide immunogen from the HER2 ECD: COOH-GCPLHNQEVTAEDGTQRC-NH2 (SEQ ID NO: 1), folded as a loop through the cysteine residues and linked to keyhole limpet hemocyanin (KLH) protein. This sequence was obtained from the NCBI database: https://www.ncbi.nlm.nih.gov/protein/NP_004439.2. This region is within domain II but is distant from the known epitope for pertuzumab (26).

Cell lines

Parental human cancer cell lines BT-474, HCC1954, MCF-7, SK-BR-3, NCI-N87, NCI-H2170, NCI-H1650, NCI-H522, and NCI-H838 were obtained from ATCC and Asterand Bioscience. The gastric cell line OE-19 was obtained from CellBank Australia. The breast cancer cell lines (BT-474, HCC1954, MCF-7, and SK-BR-3) were derived from female patients. The gastric cell lines (NCI-N87 and OE-19) and the lung cancer cell lines (NCI-H2170, NCI-H1650, NCI-H522, and NCI-H838) were all derived from male patients. Cell stocks were prepared immediately after arrival and stored by the Olivia Newton-John Cancer Research Institute central cell bank. Further cell line authentication was performed on the NCI-N87, BT-474, and HCC1954 cells in 2020 and MCF-7 in 2023 by the Queensland Institute of Medical Research via short tandem repeat profiling. Cells were used after three passages since revival from liquid nitrogen storage and within 35 passages for all experiments. Cells were routinely confirmed negative for *Mycoplasma* using a MycoAlert Mycoplasma Detection Kit (Lonza Bioscience). All cell lines were cultured at 37°C in 5% CO_2 in RPMI or DMEM/F12 (Life Technologies) supplemented with 10% FBS (Bovogen), 1% penicillin/streptomycin, and 2 mmol/L glutamine (Life Technologies). Patient-derived tumor samples were sourced from a local collaborator (Dr. Elgene Lim). These samples were obtained intraoperatively and screened for hormone receptor status and HER2 overexpression and amplification by IHC and FISH, respectively. The donor samples were treatment-naïve, and therefore, 100% tumor susceptibility to all anti-HER2 therapies was assumed. The patient derived xenograft (PDX) model generated, 14.06A.G3, was used for *in vivo* studies approved by the Austin Health Human Research Ethics Committee.

Antibodies and reagents

The recombinant HER2 ECD was provided by academic collaborator Professor A.W. Burgess (Walter and Eliza Hall Institute of Medical Research). The IgG1 idiotype antibody, LMH3 (provided by the Ludwig Institute for Cancer Research), was used as an isotype control antibody as previously described (27). Trastuzumab and pertuzumab (Genentech) were purchased.

ELISA

ELISA was performed to confirm the binding specificity to HER2-ECD of the four candidate clones designated mAb104, mAb105, mAb106, and mAb107. Briefly, polystyrene 96-well plates were precoated with 3% FCS in PBS, followed by 3 μg/mL of the linear or cyclic HER2 peptide immunogen coupled to KLH, negative control–conjugated peptide-KLH, or recombinant HER2-ECD in dilution buffer for 1 hour before 10 μg/mL antibodies were added. After a 1-hour incubation with anti-mouse IgG-alkaline phosphatase (1:3,000 dilution, Sigma-Aldrich, A3688) antibody, phosphatase activity was measured using para-nitrophenyl phosphate substrate. All incubations were performed at room temperature.

To assess the specificity of mAb104 for the HER2-ECD, polystyrene 96-well plates were coated with 3 μg/mL recombinant HER2-ECD, HER3-ECD, HER4-ECD, or EGFR-501 overnight at 4°C and blocked with 3% FCS in PBS, followed by 10 μg/mL serially diluted purified antibody along with appropriate controls for 1 hour at room temperature before anti-mouse IgG-alkaline phosphatase was added, and phosphatase activity was measured using para-nitrophenylphosphate substrate. Absorbance was measured at 405 nm using a SPECTROstar microplate reader (BMG Labtech).

Fluorescence-activated cell sorting analysis

Cells plated in a 96-well plate were incubated for 1 hour at 4°C with 10 μg/mL anti-HER2 antibodies or IgG1 isotype control antibody. Humanized antibodies, trastuzumab and pertuzumab, were detected using an Alexa Fluor 488–conjugated anti-human IgG antibody (Thermo Fisher Scientific). Bound murine antibodies were detected using an Alexa Fluor 488–conjugated anti-mouse IgG antibody.

Biosensor analysis

Surface plasmon resonance kinetic analyses were performed in a Biacore T200 system using a carboxymethyl dextran–coated sensor chip (CM5-S, GE Life Sciences). Samples of mAb104, pertuzumab, or trastuzumab were diluted to concentrations of 320 to 0 μg/mL in twofold dilution (2,133–0 nmol/L). The samples were injected at 45 μL/minute for 200 seconds (30 μL at 10 μL/minute) over the immobilized HER2-ECD. After the injection phase, the dissociation was monitored by flowing running buffer over the chip surface for 600 seconds. Bound antibody was eluted, and the chip surface was regenerated between samples by injection of 30 μL of 50 mmol/L NaOH at 30 μL/minute for 30 seconds.

Western blot analysis

Lysates of cancer cell lines were separated on 4% to 12% SDS-PAGE and immunoblotted for mAb104 and HER2. GAPDH was used as a loading control for protein normalization. Cells were treated with 100 μg/mL of antibodies for 24 hours, after which half of the wells were treated with 100 ng EGF for 10 minutes at room temperature. Total protein and MAPK activation were assessed by Western blotting using commercial antibodies against HER2 (#2242), HER2 pTyr1221/1222 (#2243), AKT (#4691), AKT pSer473 (#4060), ERK (#4695), ERK pThr202/Tyr204 (#4370), p70-S6 kinase (#2211), and pS6 (Ser 235/236; #2947), purchased from Cell Signaling Technology. The anti-GAPDH (AbC-1001) antibody was purchased from AbClon. Bands were visualized using AbSignal (AbClon, AbC-3001).

IHC of normal tissue and tumor cells and tissue

To confirm the tumor selectivity of mAb104, we evaluated a range of normal and tumor tissues for mAb104 reactivity by IHC. The staining patterns of mAb104 were compared with HER2 staining patterns using the anti-HER2 mAb, VENTANA 4B5, which is utilized

for the clinical testing of HER2 and scored using established methodologies (28–31).

Briefly, 5 μm paraffin sections were deparaffinized and rehydrated. Antigen retrieval was achieved; endogenous peroxidase and nonspecific protein-binding sites were blocked [Peroxidase Blocking Reagent (DakoCytomation); Background Sniper (Biocare)] and then incubated in mAb104 primary antibody (2.5 μg/mL for 1 hour at room temperature) and detected using streptavidin horseradish peroxidase–labeled anti-murine secondary antibody (DakoCytomation).

Human tissues were obtained from the Department of Anatomical Pathology, Austin Health, and their histologic diagnosis was confirmed by a pathologist. The IHC study was approved by the Austin Health Human Research Ethics Committee.

Biodistribution and molecular imaging studies with ^{89}Zr-labeled mAb104

NOD-SCID-IL2R$^{-/-}$ mice (Animal Research Center, Perth, Australia) with established HER2-positive NCI-N87 tumors received a trace dose of 185 kBq ^{89}Zr-DFO-mAb104 ($A_s = 37$ MBq/mg at the end of synthesis), intravenously via the tail vein (0.1 mL). On days 0 (2 hours), 1, 2, 3, 5, 7, and 9 after injection, mice ($n = 5$) were euthanized by the overinhalation of isoflurane anesthesia, and the biodistribution of radiolabeled mAb104 in normal organs and tumors was assessed. At the designated time points, the mice were humanely euthanized by isoflurane overinhalation and exsanguinated by cardiac puncture, and tumors and organs were collected immediately. All samples were counted in a dual-channel γ-scintillation counter (Wizard; PerkinElmer). Triplicate standards prepared from the injected material were counted at each time point along with tissue and tumor samples, enabling calculations to be corrected for the physical decay of the radioisotope. The tissue distribution data were calculated as the mean ± SD percentage of injected dose per gram of tissue (% ID/g) for the radiolabeled construct per time point.

In vivo PET imaging of ^{89}Zr-labeled mAb104 was performed on NOD/SCID gamma mice bearing NCI-N87 xenografts. Mice received a dose of 4.653 MBq ^{89}Zr-Df-mAb104 (126.8 μCi) and were imaged using PET and MRI on days 0 (4 hours), 2, and 7 after injection with a small-animal camera (nanoScan PET/MRI camera, Mediso).

Cell proliferation assay

Cells (1×10^4) in serum-depleted media were seeded in a 96-well microtiter plate and allowed to adhere overnight. Antibodies with appropriate controls were added with serial dilutions the following day, and one plate was harvested for a time 0 ($T = 0$) measurement. The remaining cell plates were incubated for 3 to 5 days. Cell viability was assessed using the 3-(4,5-dimethylthiazol-2-yl)-5-(3-carboxymethoxyphenyl)-2-(4-sulfophenyl)-2H-tetrazolium colorimetric viability assay with 3-(4,5-dimethylthiazol-2-yl)-5-(3-carboxymethoxyphenyl)-2-(4-sulfophenyl)-2H-tetrazolium as a substrate (Promega).

In vivo studies

NOD-SCID-IL2R$^{-/-}$ mice (Animal Resources Centre, Perth, Australia) were injected subcutaneously with 5×10^6 cells in Matrigel (BD Biosciences). Mice injected with BT-474 cells were implanted with estrogen pellets (Belma Technologies) 24 hours prior. Patient-derived tumor samples (14.06A.G3) were surgically implanted into the mammary breast pad of the mice. Tumors were allowed to grow to approximately 100 mm^3 in size, and the mice were then randomized into various treatment groups. Treatments were given three times a week at 0.5 mg of antibody per injection via intraperitoneal injections for 3 weeks. Tumor volumes were calculated using the formula $(L \times W^2)/2$, where "L" represents the larger tumor diameter and "W" the smallest tumor diameter. Tumor xenograft tissues were resected and processed as formalin-fixed, paraffin-embedded specimen sections.

All animal study protocols were approved by the Austin Health Animal Ethics Committee (protocol # A2015/05297, A2019/05605, and A2022/05790) and conducted in accordance with the Australian Code of Practice for the Care and Use of Animals for Scientific Purposes (8th Edition, 2013).

Reverse-phase protein array analysis

Protein was extracted from HER2-overexpressing NCI-N87 gastric tumors, and reverse-phase protein array analysis was performed as described previously (32, 33). In brief, tumor samples obtained at week 1 after treatment and at the end of treatment (week 3) were lysed by homogenization using RIPA lysis buffer (#9803, Cell Signaling Technology), supplemented with protease and phosphatase inhibitors (Roche Applied Science, Cat. # 05056489001). Protein concentration was normalized to 1 mg/mL as assessed using the Pierce BCA Protein Assay Kit and boiled with 2-mercaptoethanol and SDS. The protein lysates were sent to the MD Anderson Cancer Center, Houston, TX, USA, for analysis.

Internalization analysis

NCI-N87 cells were incubated with antibodies at 10 μg/mL and allowed to bind at 4°C for 1 hour prior to incubation at 37°C for the indicated times. Cells were fixed and permeabilized, and antibodies were stained with Alexa Fluor 488, LAMP1 (#9091; clone D2D11; Cell Signaling Technology), and Hoechst. Images were acquired on a Zeiss 980 inverted confocal microscope in Airyscan mode. A 405 nm diode laser was used to image Hoechst (excitation: 345 nm and emission: 478 nm), an argon laser was used to image Alexa Fluor 488 (excitation: 494 nm and emission 518 nm), and a diode laser was used for the detection of Alexa Fluor 568 (excitation: 578 nm and emission: 603 nm). Image acquisition settings (laser power, 0.2%) remained identical across all conditions and cell types. Saturation was adjusted by altering the detector gain settings. All images were subjected to Z-sectioning of 1 μm. Each image channel and slice were individually recolored, reconstructed, and processed, and isosurface rendering was performed using ZEISS ZEN Blue software (on Z slices) and ImageJ. Insets were created by zooming in on desired regions of interest (dashed lines) and performing high-resolution z-sectioning (1 μm slices) on each channel. Each image channel and slice were individually recolored, reconstructed, processed, and merged using ImageJ software. Scale bar, 20 μm. Three-dimensional surface-rendered images were created using the above z-sections of inset images and processed using the 3D isosurface rendering function on the ZEISS ZEN Blue software (Zeiss). Scale bar, 20 μm.

Statistical analysis

Analyses were performed using Prism version 9. All *P* values are two-sided, and values ≤ 0.05 were considered significant.

Data availability

The data generated in this study are available upon request from the corresponding author.

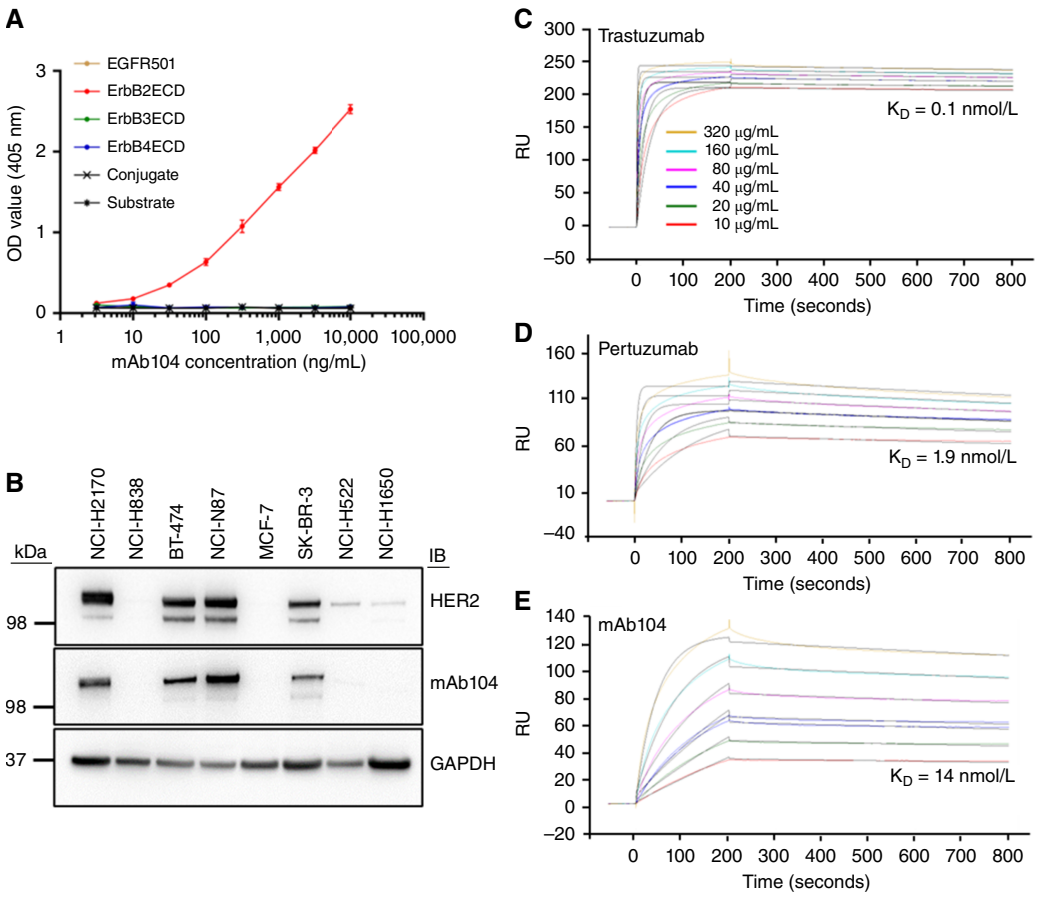

Figure 1.

Binding and specificity of mAb104. **A,** Specificity of mAb104 for the ECD of EGFR, HER2, HER3, and HER4 was evaluated using an ELISA-based assay. **B,** Western blot of mAb104 in a range of breast, gastric, and lung cancer cell lines. mAb104 binding was found only in HER2-overexpressing cell lines. GAPDH was used as a loading control. The apparent binding affinity of (**C**) trastuzumab, (**D**) pertuzumab, and (**E**) mAb104 for HER2 ECD by surface plasmon resonance (Biacore) at indicated antibody concentrations in μg/mL is shown in **C**. IB, immunoblot; OD, optical density; RU, resonance units.

Results

Binding and Specificity of mAb104

Novel HER2-targeting mAbs were generated to a conformational epitope from the HER2 ECD: H-GCPLHNQEVTAEDGTQRC-NH_2 folded as a loop through the cysteine residues and linked to KLH protein (Supplementary). The immunoglobulin isotype of the selected antibodies was detected by the Monoclonal Antibody Isotyping Kit (Thermo Fisher Scientific), and all were found to be IgG1 with K-light chains. A series of binding assays was performed, and based on the results of initial binding and affinity (K_D) measurements using Biacore analysis against the immunogen, we selected our lead candidate mAb104 for further development. Using an ELISA-based assay, mAb104 showed the strongest binding affinity to the HER2 ECD (**Fig. 1A**), as well as to the circularized and linear peptide immunogens against which the antibodies were generated (Supplementary Fig. S1). In addition, mAb104 showed the highest binding for cellular HER2 by Western blot analysis in HER2-overexpressing [defined as having an IHC score of 2+ or 3+ (34)] cancer cell lines: breast (BT-474, SK-BR-3), gastric (NCI-N87), and lung (NCI-H2170), and not in low HER2-expressing cancer cell lines: breast (MCF-7) and lung (NCI-H838, NCI-H522, and NCI-H1650; **Fig. 1B**). Subsequent analysis of binding to the HER2 ECD by surface plasmon resonance (Biacore) demonstrated high-affinity binding of mAb104 (14 nmol/L K_D) with comparable binding affinities to trastuzumab (0.1 nmol/L K_D) and pertuzumab (1.9 nmol/L K_D; **Fig. 1C–E**). As such, mAb104 was selected for further evaluation as our lead candidate.

Cell surface binding of mAb104 by FACS was compared with trastuzumab and pertuzumab in a panel of cancer cell lines with different HER2 expression levels (**Fig. 2A–D**). Of the cell lines evaluated, mAb104 showed binding to all cell lines with high HER2 expression, with the strongest binding to the HER2 population in the gastric cell line, NCI-N87, and negligible HER2 binding seen in low HER2-expressing cell lines. In all cases, mAb104 binding was consistently lower than that of pertuzumab and trastuzumab, indicating that at least *in vitro*, the mAb104 epitope is exposed in a subset of HER2 receptors (**Fig. 2**; Supplementary Fig. S2).

mAb104 binding to fixed tissue was also investigated by IHC using tissue arrays of normal and tumor tissues. In total, 11 normal human tissues and 10 common tumor types (breast intraductal carcinoma, mesothelioma, colorectal and gastric adenocarcinoma, renal cell carcinoma, lung adenocarcinoma, lung squamous cell carcinoma, hepatocellular carcinoma, prostate adenocarcinoma, and GBM) from 9 to 27 different human donors were examined

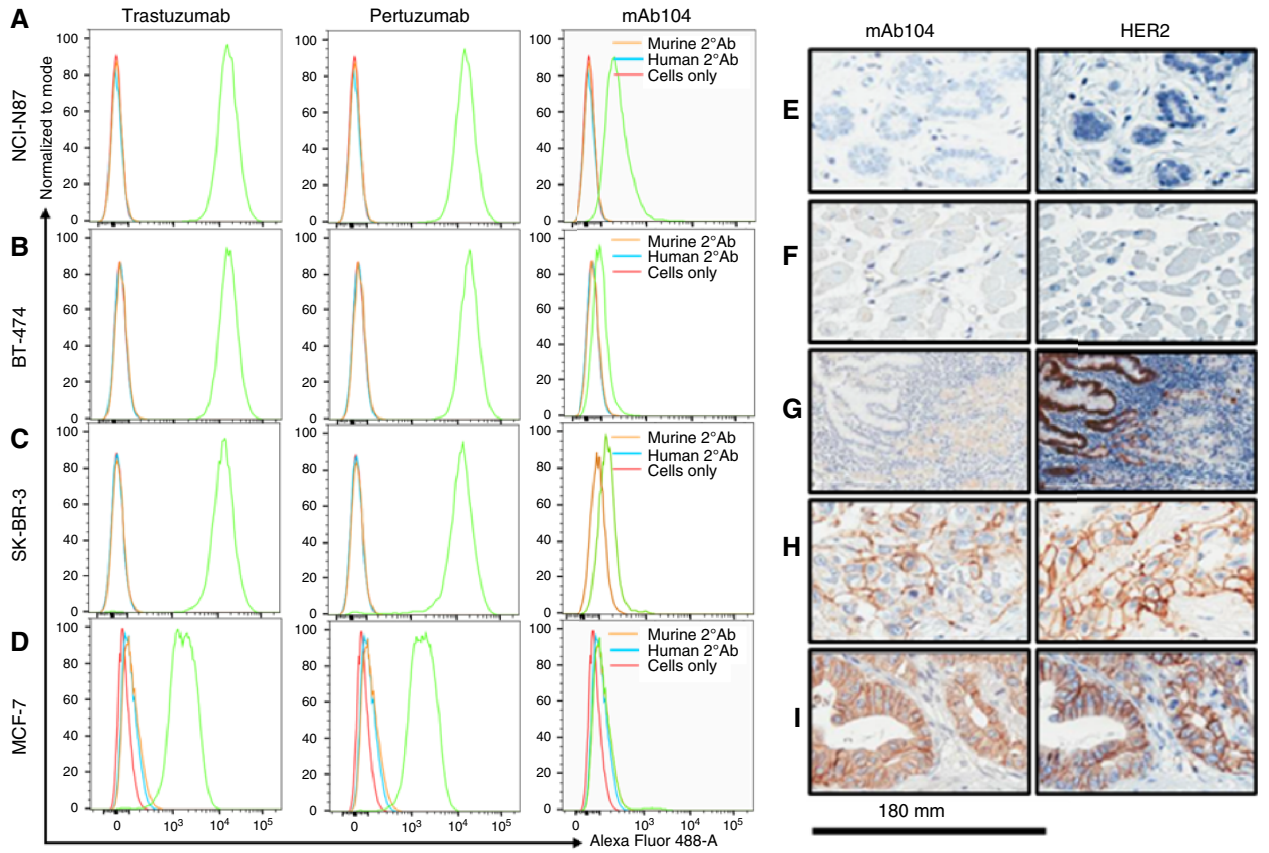

Figure 2.

FACS analysis and IHC of mAb104 binding. **A,** NCI-N87, (**B**) BT-474, (**C**) SK-BR-3, and (**D**) MCF-7 cells were incubated with 10 μg/mL trastuzumab, pertuzumab, or mAb104 (green) or secondary antibody alone (blue) or unstained (orange), and the extent of binding was determined by FACS analysis. Data are representative of two independent experiments. IHC staining with mAb104 and anti-HER2 antibody (×400): (**E**) normal breast tissue, (**F**) cardiac tissue, (**G**) stomach, (**H**) invasive ductal breast carcinoma, and (**I**) gastric cancer. Scale bar, 180 mm.

(representative data are shown in **Fig. 2E–I**; Supplementary Fig. S3). Tumor and normal tissues were not derived from the same patient (i.e., unmatched). In all cases, mAb104 showed no reactivity to normal mucosa when compared with the VENTANA FDA-approved HER2 control antibody, even in tissues in which the HER2 control antibody showed substantial binding (e.g., gastric mucosa, **Fig. 2G**). These findings suggest that despite HER2 expression, the epitope bound by mAb104 is not exposed in these tissues. In contrast, mAb104-bound HER2 in tumors with a high concordance demonstrated a relationship between mAb104 and HER2 binding in a variety of tumor types (**Fig. 2H** and **I**). The details of staining patterns and IHC scores can be found in Supplementary Tables S1 and S2.

Epitope analysis and competition assays

The 104 antibody variable domains binding the antigen epitope located on domain II of HER2 were computationally predicted from homology-modeled 3D structures of the antibody Fv domains and the known X-ray structure of human HER2 using the methods previously described (35). The predicted HER2 binding of mAb104 was compared with the known crystal structures of pertuzumab and trastuzumab binding to HER2 (**Fig. 3A**; ref. 36). The binding of mAb104 was predicted to require a conformational change that occurs upon receptor activation as previously described for EGFR (12), in which disulfide bonds of domain II of HER2 could be formed and broken dynamically based on data from the antibody mAb806.

Competition between mAb104 and pertuzumab and trastuzumab for endogenous HER2 was investigated by flow cytometry in HER2-overexpressing breast (BT-474 and SK-BR-3) and gastric (NCI-N87) cancer cell lines. These sets of experiments utilized high doses (100 μg/mL) of mAb104 preincubation to maximize the chances of seeing an impact on the binding of trastuzumab and pertuzumab. Prior incubation with a much higher dose of mAb104 did not affect trastuzumab or pertuzumab binding to cell surface HER2 (**Fig. 3B–G**). In subsequent ELISA experiments, trastuzumab and mAb104 did not affect each other's binding to HER2-ECD. Similarly, prior incubation with pertuzumab did not affect mAb104 binding; however, interestingly, prior mAb104 incubation reduced pertuzumab binding to HER2-ECD, indicating that mAb104 binding to its epitope results in steric hindrance of pertuzumab binding to its own epitope rather than actual competition for the same epitope (**Fig. 3H–J**). Discordance in the results for mAb104 competing with pertuzumab using flow cytometry and ELISA is attributed to technical differences between the antigenic preparations in the assays, that is, the presence of HER2 is in its physiologic conformation when analyzed by flow cytometry, versus partially denatured in ELISA, and consequent epitope presentation and availability.

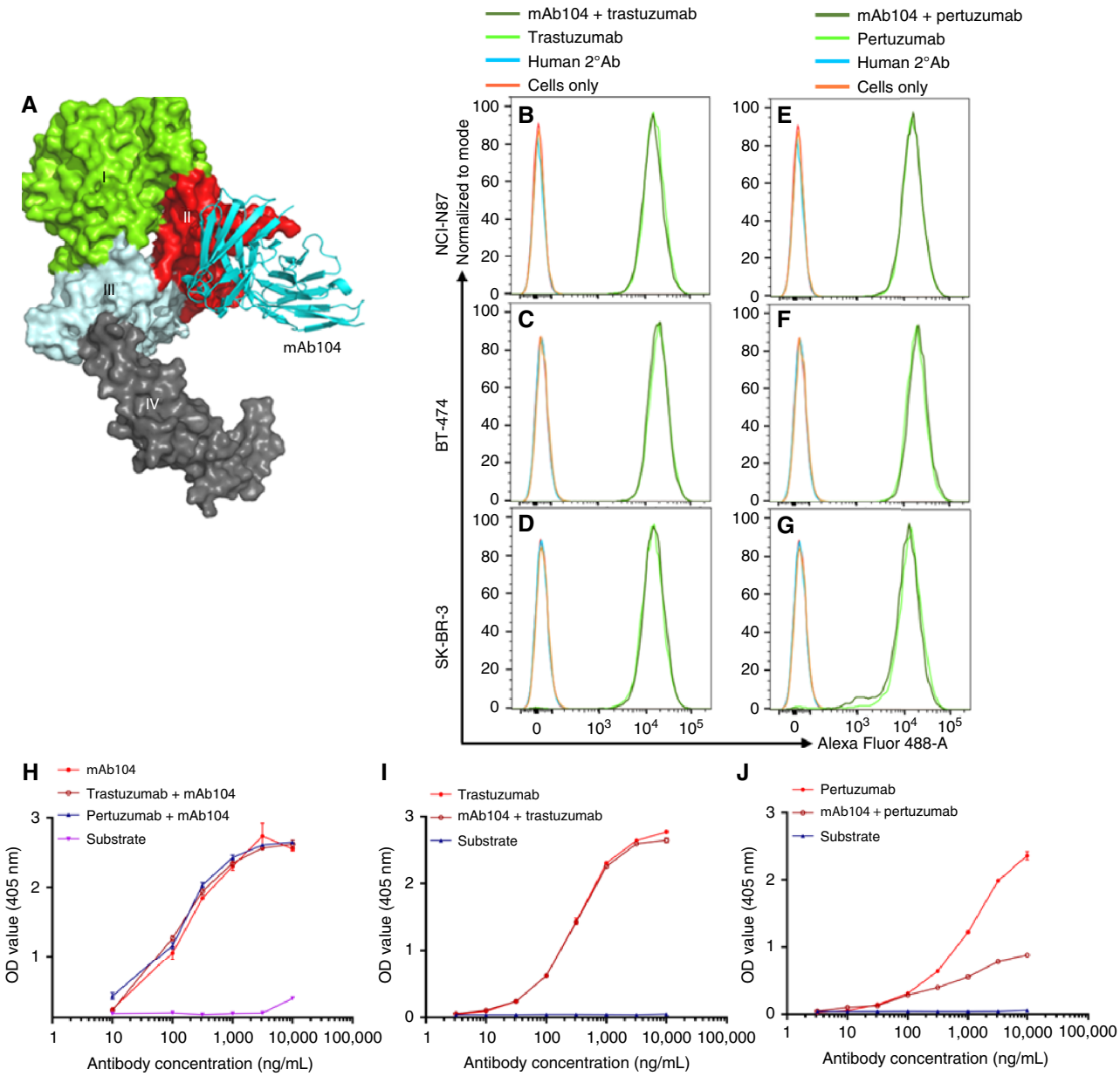

Figure 3.

Epitope analysis and competition assays. **A,** mAb104 binding to domain II of the HER2 ECD. FACS-based competition assay in which preincubation with a 10-fold excess of mAb104 (100 μg/mL) did not affect 10 μg/mL trastuzumab or pertuzumab binding, respectively, in (**B** and **E**) NCI-N87, (**C** and **F**) BT-474 cells, and (**D** and **G**) SK-BR-3 cells. ELISA-based HER2-ECD binding competition assay. **H,** Trastuzumab and pertuzumab do not affect mAb104 binding. **I,** mAb104 does not affect trastuzumab binding. **J,** mAb104 partially affects pertuzumab binding. Data are representative of two independent experiments. OD, optical density.

Effect of mAb104 on proliferation, ErbB receptors, and downstream signaling pathways *in vitro*

mAb104 as monotherapy did not demonstrate any *in vitro* activity in HER2-overexpressing breast cancer cell lines (BT-474 and SK-BR-3) and gastric cell lines [NCI-N87 and OE-19; Supplementary Fig. S4 (left)]. Furthermore, in the cell lines evaluated, the addition of mAb104 to trastuzumab did not enhance the antiproliferative effect compared with trastuzumab monotherapy [Supplementary Fig. S4 (right)]. Treatment with mAb104 in breast (SK-BR-3 and BT-474) and gastric (NCI-N87 and OE-19) cancer cell lines under ligand-independent (Supplementary Figs. S5A and S5C, S6A and S6C) and ligand-dependent (Supplementary Figs. S5B and S5D, S6A and S6D) conditions did not result in a change in the amount of total or phosphorylated HER2, nor were there any associated changes in downstream signaling.

Biodistribution studies and imaging with ^{89}Zr-labeled mAb104

Figure 4 summarizes the biodistribution results of ^{89}Zr-Df-mAb104 in HER2-positive NCI-N87 tumors in NOD/SCID gamma mice. ^{89}Zr-labeled mAb104 demonstrated high tumor uptake with

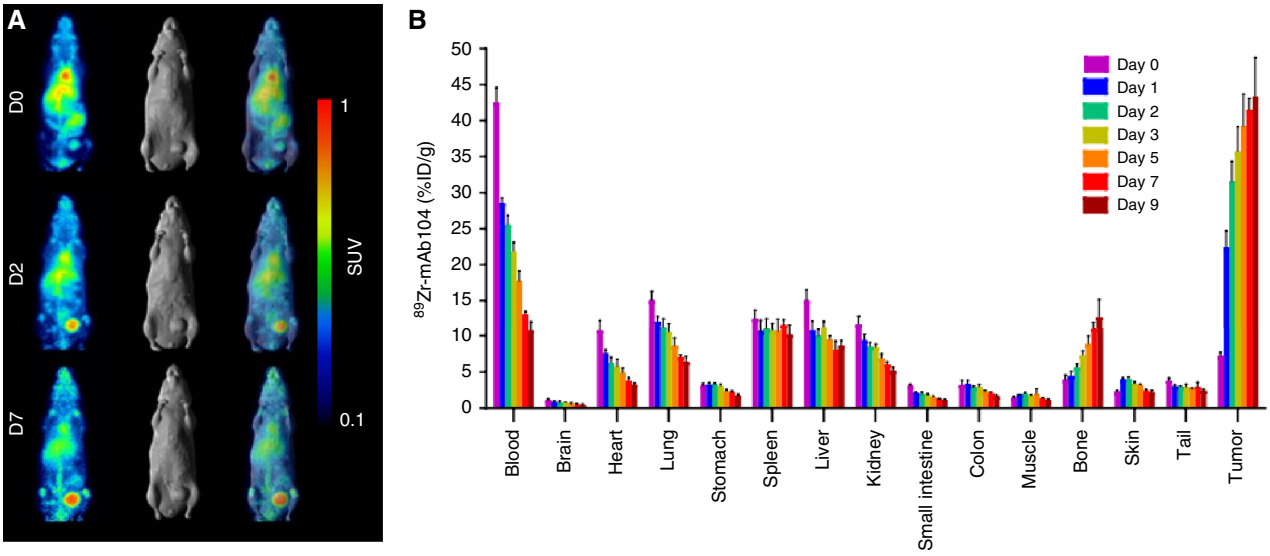

Figure 4.

Biodistribution studies and imaging with ^{89}Zr-labeled mAb104. **A,** PET (maximum intensity projection, left), surface-rendered MRI (middle), and fused PET/MRI (right) images of each NCI-N87 xenograft mouse taken on days 0, 2, and 7 after injection of ^{89}Zr-mAb104. **B,** *Ex vivo* biodistribution results showing high, specific tumor uptake of ^{89}Zr-labeled mAb104, with normal tissues demonstrating clearance patterns typical of a radiolabeled intact antibody.

some splenic and bone uptake of catabolized free ^{89}Zr but no tissue uptake in other normal organs. On day 0 (2 hours after injection), the mean ± SD levels of radioconjugate in the tumor were 7.147 ± 0.528 %ID/g, increasing to 43.310 ± 5.449 %ID/g by day 9. The tumor-to-blood ratio increased from 0.168 (day 0) to 4.036 (day 9). Whole-body PET/MR images confirmed excellent localization of ^{89}Zr-Df-mAb104 to tumors at early time points after injection (from 2 hours after injection). It was also clearly discernible that ^{89}Zr-Df-mAb104 uptake increased in tumors over time, up to 7 days after injection.

Antitumor effect of mAb104 *in vivo*

The therapeutic efficacy of mAb104 was evaluated *in vivo* in a variety of tumor xenograft models as well as one breast PDX model cell line, both as monotherapy and in combination with trastuzumab (**Fig. 5**). In view of the potential steric hindrance of pertuzumab binding due to mAb104, the combination of mAb104 and pertuzumab *in vivo* was not tested. Treatment with mAb104 as monotherapy resulted in significant tumor growth inhibition in BT-474 (**Fig. 5B**) xenografts as well as in a HER2-positive breast 14.06A.G3 PDX model (**Fig. 5C**) compared with the control isotype antibody and demonstrated equivalent efficacy to trastuzumab and pertuzumab monotherapy, with no significant differences between the treatment arms. Similarly, in the gastric NCI-N87 (**Fig. 5A**) and OE-19 (Supplementary Fig. S7B and S7C) xenograft models, mAb104 also showed significant antitumor activity as monotherapy. No statistical difference in growth inhibition was seen between mAb104 and trastuzumab or pertuzumab. However, in OE-19 tumors, trastuzumab was significantly more efficacious than both pertuzumab ($P = 0.024$) and mAb104 ($P = 0.004$; Supplementary Fig. S7B and S7C).

In all *in vivo* models, treatment with mAb104 in combination with trastuzumab resulted in significantly greater tumor reduction compared with trastuzumab alone and similar tumor inhibition to trastuzumab and pertuzumab (**Fig. 5D–F**; Supplementary Fig. S7B and S7C).

Effect of mAb104 on downstream signaling pathways *in vivo*

Tumors taken at weeks 1 and 3 of treatment were analyzed by Western blot for effects on HER2 and known HER2-activated signaling pathways. Treatment with mAb104 resulted in the reduction of total HER2 and phosphorylated HER2 expression, similar to trastuzumab. There was also marked inhibition of the mTOR signaling pathway, with decreases in both phosphorylated and total mTOR levels, and also downstream mTOR targets such as phosphorylated ribosomal protein S6 and p21 (Supplementary Fig. S8). This signaling does not seem to be mediated through the canonical AKT/mTOR signaling pathway because the levels of phosphorylated and total AKT do not seem to be inhibited.

Internalization

ErbB receptors are internalized into cells following homo-/heterodimerization, with kinase activation and signaling typically occurring during the ErbB receptor (or antibody:ErbB receptor) trafficking into endosomes (1). We examined the internalization of mAb104 following binding to NCI-N87 cells by confocal microscopy. mAb104 showed relatively rapid internalization by 6 hours (**Fig. 6**).

Discussion

HER2 remains a critical oncogene, biomarker, and target in many tumor types. However, despite the success of current HER2 antibodies, resistance invariably develops. In this context, new strategies to target HER2 are clearly needed and remain a priority. mAb104 binds to domain II of the HER2-ECD with high affinity and exhibits potent antitumor activity in HER2-overexpressing xenografts and PDX models. Competition assays demonstrate that the mAb104 epitope is clearly

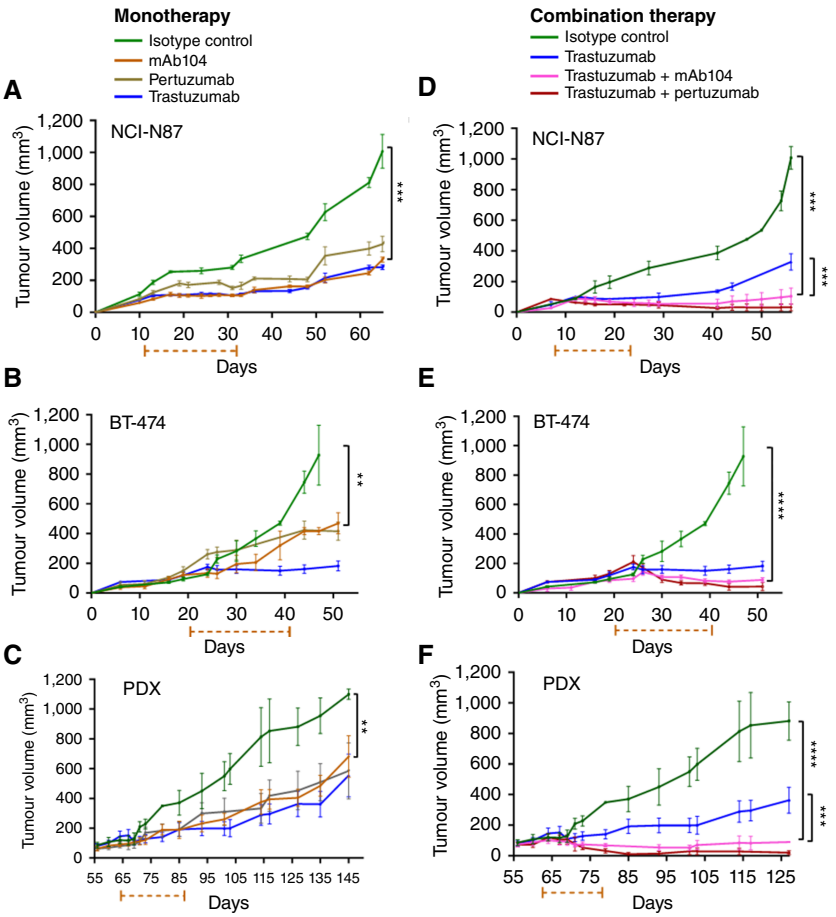

Figure 5.

Antitumor effects of mAb104 in HER2-overexpressing tumor models. A total of 0.5 mg of trastuzumab, pertuzumab, or mAb104 was administered thrice per week for 3 weeks (indicated by the broken orange line) as monotherapy (left) or in combination (right) in mice ($n = 5$) bearing xenografts of (**A** and **D**) gastric tumor NCI-N87, (**B** and **E**) breast tumor BT-474, and (**C** and **F**) HER2-positive breast PDX model. Data shown in the growth curve represent mean tumor volume ± SE. **, $P < 0.01$; ***, $P < 0.001$; ****, $P < 0.0001$.

different from trastuzumab and also from pertuzumab despite both mAb104 and pertuzumab targeting domain II of HER2. The mAb104 epitope was not evident in low HER2-expressing cell lines, which we hypothesize is due to the lack of altered conformational states of HER2 in conditions in which the basal activation is minimal.

mAb104 showed no significant binding to normal tissue, and importantly, no binding was observed in tissues in which the control HER2 antibody had positive staining, that is, gastric mucosa and renal tissue. Of note was that the control HER2 antibody binds to the same epitope as trastuzumab, and the results indicate that mAb104 will have less normal tissue binding than trastuzumab. This is consistent with conclusions that the epitope bound by mAb104 is not constitutively exposed in normal tissues. Trastuzumab has been shown to cause cardiotoxicity, a severe and dose-limiting toxicity, requiring routine cardiac monitoring (37). Notably, mAb104 had no staining in cardiac tissue. Despite this, we found binding of mAb104 to tumor cells with high HER2 expression/amplification with an intensity of staining comparable with that of the HER2 control antibody. In addition, the biodistribution data demonstrated that the uptake of ^{89}Zr-Df-mAb104 was compared with ^{89}Zr-radiolabeled trastuzumab and pertuzumab (38–41). These tissue screening data, combined with the biodistribution and imaging patterns and the epitope and modeling studies, indicate that mAb104 binds to a tumor-specific form of HER2 and, therefore, leads to reduced toxicity compared with current HER2 antibodies.

mAb104 had no detectable effect *in vitro*, which is consistent with other studies that evaluated antibodies targeting conformationally exposed epitopes on the EGFR (42–44) and suggests that the dynamic turnover of HER2 or other factors *in vivo* are required for the functional effects of mAb104 on HER2 function. Despite the lack of *in vitro* activity, mAb104 demonstrated a potent antitumor effect *in vivo* in a range of HER2-overexpressing xenograft and PDX models. The antitumor effects of mAb104 as a single agent *in vivo* are comparable with those of trastuzumab and pertuzumab in most models. mAb104 in combination with trastuzumab is significantly more potent than trastuzumab monotherapy and has similar antitumor effects to combined trastuzumab and pertuzumab. These findings are supported by reports that show combining antibodies that target distinct nonoverlapping epitopes of HER2 increases antitumor activity (45) and our own demonstration of similar results with antibodies against EGFR (46). We hypothesize that the discrepancy between the lack of *in vitro* effects and the potent *in vivo* activity of mAb104 is likely due to the altered activation of the HER2 receptor and the turnover rate and internalization kinetics of HER2 *in vivo* compared with *in vitro*. It can, therefore, be postulated that *in vitro* studies do not optimally examine the mechanisms, which underlie the activity of this class of antibodies.

HER2 overexpression is associated with an increase in the expression of variants of HER2, and the increase in each of these may be functionally relevant to cell proliferation and transformation (47). Differential responses of HER2-amplified cells to anti-HER2

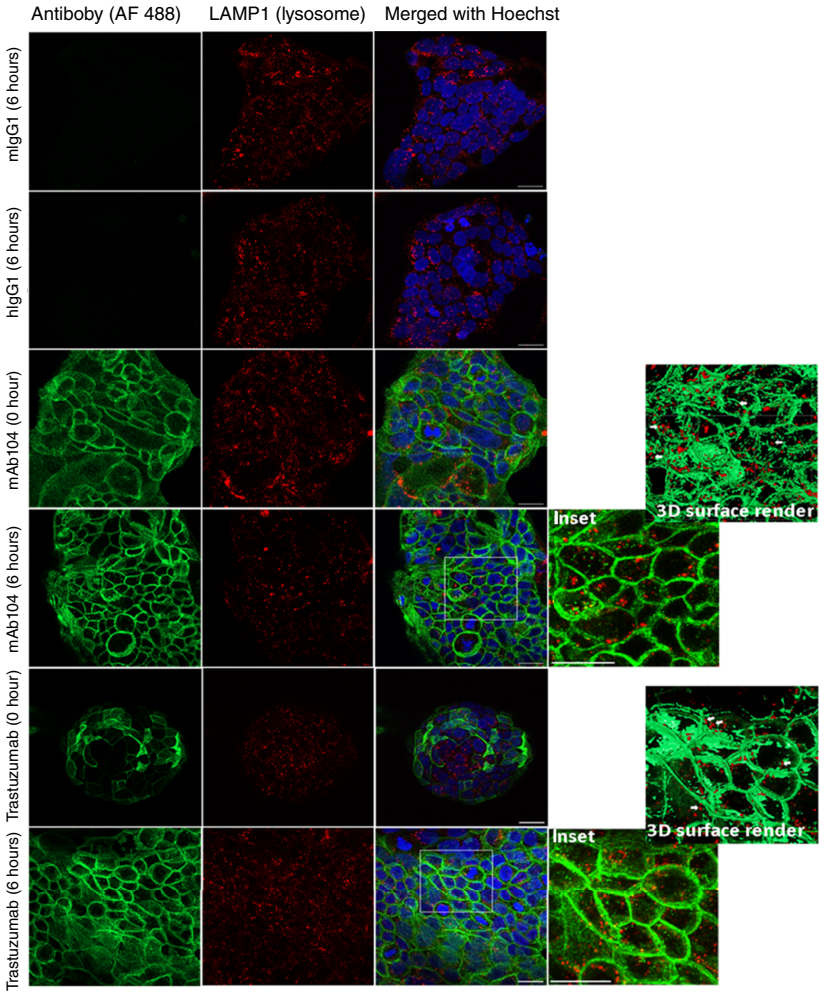

Figure 6.
Internalization assay. mAb104-HER2 receptor complexes are internalized in NCI-N87 cells and engage with lysosomes. mAb104 was detected using Alexa Fluor 488 (AF 488; green). Cells were counterstained with LAMP1 (red; lysosomes) and Hoechst (blue; nucleus). All images are Z-projections of 1 μm sections. Arrows indicate antibody–receptor engagement with lysosomes. Insets: high-resolution scan of dashed line region. The red/green channels are z-sectioned (1 μm), individually recolored, reconstructed, processed, and merged. 3D render: 3D isosurface render of z-sectioned insets preformed using ZEISS ZEN Blue software. Scale bar, 20 μm. Magnification 250×.

therapies have been shown to be highly dependent on the tumor microenvironment, which can influence the activation of downstream pathways, such as the PI3K-AKT and RAS-MAPK pathways (48). We have shown that mAb104 specifically binds to HER2 and postulate that mAb104 potentially exerts its antitumor effects by inhibiting HER2-mediated signaling directly and AKT/mTOR signaling through noncanonical pathways. The effect of trastuzumab on HER2 dimerization and on the MAPK and other signaling pathways is not fully understood (49). Various studies have shown that trastuzumab can inhibit or activate the MAPK pathway depending on the conditions and cell lines used as well as the duration of drug exposure (50–54).

Despite resistance to anti-HER2 therapies occurring almost universally, tumors continue to remain "addicted" to HER2 signaling, and therefore, the development of novel therapies remains critical in this area of unmet need. In contrast to other reported tumor-specific HER2 antibodies (55), mAb104 has shown potent antitumor effects in a variety of xenograft and PDX models, tumor specificity, and lack of normal tissue binding, as well as the ability to internalize in tumor cells. These characteristics strongly support the development of mAb104 as a naked antibody but also for payload delivery as an ADC for β/αparticle therapy, in which the lack of normal tissue binding has great potential for minimizing toxicity while enhancing tumor therapeutic efficacy.

Authors' Disclosures

S. Parakh reports a patent for WO2020191434 issued. I.J.G. Burvenich reports grants from the National Imaging Facility and the National Health and Medical Research Council (NHMRC) during the conduct of the study. C.W. Wichmann reports other support from Telix Pharmaceuticals Ltd and Clarity Pharmaceuticals Ltd and grants from Telix Pharmaceuticals Ltd outside the submitted work. H.K. Gan reports grants from the NHMRC during the conduct of the study and has a patent for WO2020191434 issued. A.M. Scott reports grants from the NHMRC during the conduct of the study as well as grants and other support from Telix Pharmaceuticals and Avid Radiopharmaceuticals, grants from Antengene and Humanigen, and other support from ImaginAb, ITM, Fusion Pharmaceuticals, and Cyclotek outside the submitted work and has a patent for mAb104 issued and licensed and is the founder of Certis Therapeutics. No disclosures were reported by the other authors.

Authors' Contributions

S. Parakh: Conceptualization, formal analysis, methodology, writing–original draft, writing–review and editing. **N. Huynh:** Formal analysis, investigation, writing–review and editing. **D.D. Cao:** Investigation, writing–review and editing. **A. Rigopoulos:** Investigation, writing–review and editing. **B. Gloria:** Methodology, writing–review and editing. **I.J.G. Burvenich:** Investigation, writing–review and editing. **C. Murone:** Investigation. **C.W. Wichmann:** Methodology, writing–review and editing. **N.Y. Guo:** Investigation, writing–review and editing. **C. Senko:** Methodology, writing–review and editing. **A. Parslow:** Investigation. **L. Allan:** Investigation, writing–review and editing. **L.D. Osellame:** Investigation, writing–

review and editing. **P.W. Janes:** Formal analysis, investigation, writing–review and editing. **F.E. Scott:** Project administration, writing–review and editing. **Z. Liu:** Supervision, methodology, writing–review and editing. **H.K. Gan:** Supervision, methodology, project administration, writing–review and editing. **A.M. Scott:** Conceptualization, resources, supervision, funding acquisition, project administration, writing–review and editing.

Acknowledgments

A.M. Scott was supported by an NHMRC Investigator grant (No. 1177837). S. Parakh is supported by a VCA Fellowship grant (No. ECRF20010). We acknowledge the Australian Cancer Research Foundation for providing funds to purchase the nanoPET/MRI and nanoSPECT/CT imaging equipment. The support of the Operational Infrastructure Support Program of the Victorian State Government is acknowledged, and this research was also undertaken using the Solid Target Laboratory, an ANSTO-Austin-ONJCRI Partnership. The authors acknowledge the facilities and scientific and technical assistance of the National Imaging Facility (I.J.G. Burvenich, National Imaging Facility fellow), a National Collaborative Research Infrastructure Strategy capability, at the La Trobe-ONJCRI facility.

Note

Supplementary data for this article are available at Molecular Cancer Therapeutics Online (http://mct.aacrjournals.org/).

Received July 15, 2024; revised December 13, 2024; accepted May 8, 2025; posted first May 13, 2025.

References

1. Parakh S, Gan HK, Parslow AC, Burvenich IJG, Burgess AW, Scott AM. Evolution of anti-HER2 therapies for cancer treatment. Cancer Treat Rev 2017;59:1–21.
2. Klapper LN, Glathe S, Vaisman N, Hynes NE, Andrews GC, Sela M, et al. The ErbB-2/HER2 oncoprotein of human carcinomas may function solely as a shared coreceptor for multiple stroma-derived growth factors. Proc Natl Acad Sci U S A 1999;96:4995–5000.
3. Maruyama IN. Mechanisms of activation of receptor tyrosine kinases: monomers or dimers. Cells 2014;3:304–30.
4. Hudziak RM, Schlessinger J, Ullrich A. Increased expression of the putative growth factor receptor p185HER2 causes transformation and tumorigenesis of NIH 3T3 cells. Proc Natl Acad Sci U S A 1987;84:7159–63.
5. Chazin V, Kaleko M, Miller A, Slamon D. Transformation mediated by the human HER-2 gene independent of the epidermal growth factor receptor. Oncogene 1992;7:1859–66.
6. Woods Ignatoski KM, Grewal NK, Markwart S, Livant DL, Ethier SP. p38MAPK induces cell surface alpha4 integrin downregulation to facilitate erbB-2-mediated invasion. Neoplasia 2003;5:128–34.
7. Benz CC, Scott GK, Sarup JC, Johnson RM, Tripathy D, Coronado E, et al. Estrogen-dependent, tamoxifen-resistant tumorigenic growth of MCF-7 cells transfected with HER2/neu. Breast Cancer Res Treat 1992;24:85–95.
8. Adams CW, Allison DE, Flagella K, Presta L, Clarke J, Dybdal N, et al. Humanization of a recombinant monoclonal antibody to produce a therapeutic HER dimerization inhibitor, pertuzumab. Cancer Immunol Immunother 2006;55:717–27.
9. Ko B-K, Lee S-Y, Lee Y-H, Hwang I-S, Persson H, Rockberg J, et al. Combination of novel HER2-targeting antibody 1E11 with trastuzumab shows synergistic antitumor activity in HER2-positive gastric cancer. Mol Oncol 2015;9:398–408.
10. Mahdavi M, Keyhanfar M, Jafarian A, Mohabatkar H, Rabbani M. Production and characterization of new anti-HER2 monoclonal antibodies. Monoclon Antib Immunodiagn Immunother 2015;34:213–21.
11. Ceran C, Cokol M, Cingoz S, Tasan I, Ozturk M, Yagci T. Novel anti-HER2 monoclonal antibodies: synergy and antagonism with tumor necrosis factor-α. BMC Cancer 2012;12:450.
12. Garrett TP, Burgess AW, Gan HK, Luwor RB, Cartwright G, Walker F, et al. Antibodies specifically targeting a locally misfolded region of tumor associated EGFR. Proc Natl Acad Sci U S A 2009;106:5082–7.
13. Johns TG, Adams TE, Cochran JR, Hall NE, Hoyne PA, Olsen MJ, et al. Identification of the epitope for the epidermal growth factor receptor-specific monoclonal antibody 806 reveals that it preferentially recognizes an untethered form of the receptor. J Biol Chem 2004;279:30375–84.
14. Scott AM, Lee F-T, Tebbutt N, Herbertson R, Gill SS, Liu Z, et al. A phase I clinical trial with monoclonal antibody ch806 targeting transitional state and mutant epidermal growth factor receptors. Proc Natl Acad Sci U S A 2007;104:4071–6.
15. Cleary JM, Yee LK-C, Azad N, Carducci M, Cosgrove D, Limaye S, et al. Abstract 2506: a phase 1 study of ABT-806, a humanized recombinant anti-EGFR monoclonal antibody, in patients with advanced solid tumors. Cancer Res 2012;72(Suppl 8):2506.
16. Gan HK, Burge M, Solomon B, Lee ST, Holen KD, Zhang Y, et al. A phase 1 and biodistribution study of ABT-806i, an 111In-radiolabeled conjugate of the tumor-specific anti-EGFR antibody ABT-806. J Nucl Med 2021;62:787–94.
17. Doronina SO, Bovee TD, Meyer DW, Miyamoto JB, Anderson ME, Morris-Tilden CA, et al. Novel peptide linkers for highly potent antibody− auristatin conjugate. Bioconjug Chem 2008;19:1960–3.
18. Reardon DA, Lassman AB, van den Bent M, Kumthekar P, Merrell R, Scott AM, et al. Efficacy and safety results of ABT-414 in combination with radiation and temozolomide in newly diagnosed glioblastoma. Neuro Oncol 2017;19:965–75.
19. Lassman AB, Van Den Bent MJ, Gan HK, Reardon DA, Kumthekar P, Butowski N, et al. Safety and efficacy of depatuxizumab mafodotin + temozolomide in patients with EGFR-amplified, recurrent glioblastoma: results from an international phase I multicenter trial. Neuro Oncol 2019;21:106–14.
20. Lassman AB, Pugh SL, Wang TJC, Aldape K, Gan HK, Preusser M, et al. Depatuxizumab mafodotin (ABT-414) in EGFR-amplified newly diagnosed GBM: a randomized, double-blind, phase III, international clinical trial. In: Annual Meeting of the Society for Neuro-Oncology; Phoenix (AZ); 2019.
21. Van Den Bent MJ, French P, Eoli M, Sepúlveda JM, Walenkamp AME, Frenel J-S, et al. Updated results of the INTELLANCE 2/EORTC trial 1410 randomized phase II study on Depatux–M alone, Depatux-M in combination with temozolomide (TMZ) and either TMZ or lomustine (LOM) in recurrent EGFR amplified glioblastoma (NCT02343406). J Clin Oncol 2018;36(Suppl 15):2023.
22. van den Bent M, Eoli M, Sepulveda JM, Smits M, Walenkamp A, Frenel J-S, et al. Ltbk-04 first results of the randomized phase ii study on depatux–M alone, depatux-M in combination with temozolomide and either temozolomide or lomustine in recurrent egfr amplified glioblastoma: first report from intellance 2/eortc trial 1410. Neuro Oncol 2017;19(Suppl 6):vi316.
23. Carneiro BA, Bestvina CM, Shmueli ES, Gan HK, Beck JT, Robinson R, et al. Phase I study of the antibody-drug conjugate ABBV-321 in patients with non-small cell lung cancer and squamous head and neck cancer with overexpression of the epidermal growth factor receptor. J Clin Oncol 2020;38(Suppl 15):TPS3649.
24. Phillips AC, Boghaert ER, Vaidya KS, Falls HD, Mitten MJ, DeVries PJ, et al. Characterization of ABBV-221, a tumor-selective EGFR targeting antibody drug conjugate. Mol Cancer Ther 2018:17;795–805.
25. Rotow J, Yoh K, Powderly J, Shimizu T, Perets R, Paz-Ares L, et al. 1185TiP First-in-human phase I study of ABBV-637 as monotherapy and in combination in patients with relapsed and refractory solid tumors. Ann Oncol 2022;33(Suppl 7):S1090.
26. Franklin MC, Carey KD, Vajdos FF, Leahy DJ, De Vos AM, Sliwkowski MX. Insights into ErbB signaling from the structure of the ErbB2-pertuzumab complex. Cancer Cell 2004;5:317–28.
27. Liu Z, Panousis C, Smyth FE, Murphy R, Wirth V, Cartwright G, et al. Generation of anti-idiotype antibodies for application in clinical immunotherapy laboratory analyses. Hybrid Hybridomics 2003;22:219–28.
28. Wolff AC, Hammond MEH, Hicks DG, Dowsett M, McShane LM, Allison KH, et al. Recommendations for human epidermal growth factor receptor 2 testing in breast cancer: American Society of Clinical Oncology/College of American Pathologists clinical practice guideline update. J Clin Oncol 2013;31:3997–4013.
29. Hofmann M, Stoss O, Shi D, Büttner R, Van De Vijver M, Kim W, et al. Assessment of a HER2 scoring system for gastric cancer: results from a validation study. Histopathology 2008;52:797–805.
30. Bang Y-J, Van Cutsem E, Feyereislova A, Chung HC, Shen L, Sawaki A, et al. Trastuzumab in combination with chemotherapy versus chemotherapy alone

for treatment of HER2-positive advanced gastric or gastro-oesophageal junction cancer (ToGA): a phase 3, open-label, randomised controlled trial. Lancet 2010;376:687–97.
31. Rüschoff J, Dietel M, Baretton G, Arbogast S, Walch A, Monges G, et al. HER2 diagnostics in gastric cancer—guideline validation and development of standardized immunohistochemical testing. Virchows Arch 2010;457:299–307.
32. Elster N, Cremona M, Morgan C, Toomey S, Carr A, O'Grady A, et al. A preclinical evaluation of the PI3K alpha/delta dominant inhibitor BAY 80 to 6946 in HER2-positive breast cancer models with acquired resistance to the HER2-targeted therapies trastuzumab and lapatinib. Breast Cancer Res Treat 2015;149:373–83.
33. Hennessy BT, Lu Y, Gonzalez-Angulo AM, Carey MS, Myhre S, Ju Z, et al. A technical assessment of the utility of reverse phase protein arrays for the study of the functional proteome in non-microdissected human breast cancers. Clin Proteomics 2010;6:129–51.
34. Viale GO. HER2 in breast cancer: ESMO biomarker factsheet.
35. Zhang W, Zeng X, Zhang L, Peng H, Jiao Y, Zeng J, et al. Computational identification of epitopes in the glycoproteins of novel bunyavirus (SFTS virus) recognized by a human monoclonal antibody (MAb 4–5). J Comput Aided Mol Des 2013;27:539–50.
36. Hu S, Sun Y, Meng Y, Wang X, Yang W, Fu W, et al. Molecular architecture of the ErbB2 extracellular domain homodimer. Oncotarget 2015;6:1695–706.
37. Copeland-Halperin RS, Liu JE, Yu AF. Cardiotoxicity of HER2-targeted therapies. Curr Opin Cardiol 2019;34:451–8.
38. Chang AJ, DeSilva R, Jain S, Lears K, Rogers B, Lapi S. 89Zr-radiolabeled trastuzumab imaging in orthotopic and metastatic breast tumors. Pharmaceuticals 2012;5:79–93.
39. Mohammadpour-Ghazi F, Yousefnia H, Divband G, Zolghadri S, Alirezapour B, Shakeri F. Development and evaluation of ^{89}Zr-trastuzumab for clinical applications. Asia Ocean J Nucl Med Biol 2023;11:135–44.
40. Kang M, Shin JI, Han S, Kim JY, Park J, Kim KI, et al. Therapeutic response monitoring with ^{89}Zr-DFO-pertuzumab in HER2-positive and trastuzumab-resistant breast cancer models. Pharmaceutics 2022;14:1338.
41. Marquez BV, Ikotun OF, Zheleznyak A, Wright B, Hari-Raj A, Pierce RA, et al. Evaluation of 89Zr-pertuzumab in breast cancer xenografts. Mol Pharm 2014;11:3988–95.
42. Gan HK, Burgess AW, Clayton AHA, Scott AM. Targeting of a conformationally exposed, tumor-specific epitope of EGFR as a strategy for cancer therapy. Cancer Res 2012;72:2924–30.
43. Johns TG, Luwor RB, Murone C, Walker F, Weinstock J, Vitali AA, et al. Antitumor efficacy of cytotoxic drugs and the monoclonal antibody 806 is enhanced by the EGF receptor inhibitor AG1478. Proc Natl Acad Sci U S A 2003;100:15871–6.
44. Johns TG, Perera RM, Vernes SC, Vitali AA, Cao DX, Cavenee WK, et al. The efficacy of epidermal growth factor receptor–specific antibodies against glioma xenografts is influenced by receptor levels, activation status, and heterodimerization. Clin Cancer Res 2007;13:1911–25.
45. Zhang A, Shen G, Zhao T, Zhang G, Liu J, Song L, et al. Augmented inhibition of angiogenesis by combination of HER2 antibody chA21 and trastuzumab in human ovarian carcinoma xenograft. J Ovarian Res 2010;3:20.
46. Perera RM, Narita Y, Furnari FB, Gan HK, Murone C, Ahlkvist M, et al. Treatment of human tumor xenografts with monoclonal antibody 806 in combination with a prototypical epidermal growth factor receptor–specific antibody generates enhanced antitumor activity. Clin Cancer Res 2005;11:6390–9.
47. Moasser MM. The oncogene HER2: its signaling and transforming functions and its role in human cancer pathogenesis. Oncogene 2007;26:6469–87.
48. Weigelt B, Lo AT, Park CC, Gray JW, Bissell MJ. HER2 signaling pathway activation and response of breast cancer cells to HER2-targeting agents is dependent strongly on the 3D microenvironment. Breast Cancer Res Treat 2010;122:35–43.
49. Nami B, Maadi H, Wang Z. Mechanisms underlying the action and synergism of trastuzumab and pertuzumab in targeting HER2-positive breast cancer. Cancers (Basel) 2018;10:342.
50. Dokmanovic M, Wu Y, Shen Y, Chen J, Hirsch DS, Wu WJ. Trastuzumab-induced recruitment of Csk-homologous kinase (CHK) to ErbB2 receptor is associated with ErbB2-Y1248 phosphorylation and ErbB2 degradation to mediate cell growth inhibition. Cancer Biol Ther 2014;15:1029–41.
51. Bagnato P, Castagnino A, Cortese K, Bono M, Grasso S, Bellese G, et al. Cooperative but distinct early co-signaling events originate from ERBB2 and ERBB1 receptors upon trastuzumab treatment in breast cancer cells. Oncotarget 2017;8:60109–22.
52. Yu X, Wang L, Shen Y, Wang C, Zhang Y, Meng Y, et al. Targeting EGFR/HER2 heterodimerization with a novel anti-HER2 domain II/III antibody. Mol Immunol 2017;87:300–7.
53. Yakes FM, Chinratanalab W, Ritter CA, King W, Seelig S, Arteaga CL. Herceptin-induced inhibition of phosphatidylinositol-3 kinase and Akt Is required for antibody-mediated effects on p27, cyclin D1, and antitumor action. Cancer Res 2002;62:4132–41.
54. Ghosh R, Narasanna A, Wang SE, Liu S, Chakrabarty A, Balko JM, et al. Trastuzumab has preferential activity against breast cancers driven by HER2 homodimers. Cancer Res 2011;71:1871–82.
55. Arimori T, Mihara E, Suzuki H, Ohishi T, Tanaka T, Kaneko MK, et al. Locally misfolded HER2 expressed on cancer cells is a promising target for development of cancer-specific antibodies. Structure 2024;32:536–49.e5.